

# The characteristics of ZnO–Bi<sub>2</sub>O<sub>3</sub>-based varistor ceramics doped with Y<sub>2</sub>O<sub>3</sub> and varying amounts of Sb<sub>2</sub>O<sub>3</sub>

Slavko Bernik<sup>a,\*</sup>, Srečo Maček<sup>a</sup>, Ai Bui<sup>b</sup>

<sup>a</sup>Jožef Stefan Institute, Jamova 39, 1000 Ljubljana, Slovenia

<sup>b</sup>Universite Paul Sabatier, Laboratoire de Genie Electrique, 118 Route de Narbonne, Toulouse, France

## Abstract

ZnO–Bi<sub>2</sub>O<sub>3</sub>-based varistor samples doped with 0.45 mol% of Y<sub>2</sub>O<sub>3</sub> and varying amounts of Sb<sub>2</sub>O<sub>3</sub> in the range from 1.8 to 0.0 mol% were fired at 1230 °C. Only in the samples co-doped with Sb<sub>2</sub>O<sub>3</sub> did doping with Y<sub>2</sub>O<sub>3</sub> resulted in the formation of a fine-grained Bi–Zn–Sb–Y–O phase (the Y<sub>2</sub>O<sub>3</sub>-containing phase) at the grain boundaries, which very effectively hinders the grain growth. Despite of a decrease in the amount of added Sb<sub>2</sub>O<sub>3</sub> from 1.8 to 0.45 mol% and a significant decrease in the amount of spinel phase the samples had a similar ZnO grain size and a threshold voltage of 200 V/mm. The results confirmed that doping with Y<sub>2</sub>O<sub>3</sub> is a very promising route for the production of fine-grained high-voltage ZnO–Bi<sub>2</sub>O<sub>3</sub>-based varistor ceramics, and determining the proper amounts of added Sb<sub>2</sub>O<sub>3</sub> and Y<sub>2</sub>O<sub>3</sub> is of great importance.

© 2003 Elsevier Ltd. All rights reserved.

**Keywords:** Electrical properties; Grain size; Microstructure-final; Varistor; ZnO

## 1. Introduction

As the non-linear current-voltage characteristic of ZnO-based varistor ceramics<sup>1</sup> is a grain-boundary phenomenon, with the breakdown voltage of the non-ohmic grain boundary at 3 V, the ZnO grain size is directly related to the electrical characteristics of the varistor. Hence, tailoring of the ZnO grain size is essential for controlling the breakdown voltage of varistor ceramics. The composition of varistor ceramics is rather complex, composed mainly of ZnO to which small amounts of oxides such as Bi<sub>2</sub>O<sub>3</sub>, Sb<sub>2</sub>O<sub>3</sub>, Co<sub>3</sub>O<sub>4</sub>, Mn<sub>3</sub>O<sub>4</sub>, Cr<sub>2</sub>O<sub>3</sub> and others are added. Sb<sub>2</sub>O<sub>3</sub> is generally considered as the grain-growth-controlling dopant since its addition results in the formation of the Zn<sub>7</sub>Sb<sub>2</sub>O<sub>12</sub> spinel-type phase that reduces the mobility of grain boundaries and hence hinders the grain growth.<sup>2</sup> Sb<sub>2</sub>O<sub>3</sub> also results in the formation of so-called inversion boundaries (IBs) in practically every ZnO grain of the varistor ceramics. Daneu et al.<sup>3</sup> revealed their influence on the grain growth and the possibility to tailor the ZnO grain size with an IBs-induced grain-growth mechanism

was confirmed in the ZnO ceramics doped with small amounts of Sb<sub>2</sub>O<sub>3</sub>.<sup>4</sup> It has been reported recently that the breakdown voltage and the energy characteristics of varistor ceramics can also be significantly increased by doping with rare-earth oxides.<sup>5</sup> Reports on Y<sub>2</sub>O<sub>3</sub>-doped<sup>6</sup> as well as Pr<sub>6</sub>O<sub>11</sub>- and Nd<sub>2</sub>O<sub>3</sub>-doped<sup>7</sup> ZnO–Bi<sub>2</sub>O<sub>3</sub>-based varistor ceramics have confirmed the possibility of preparing fine-grained varistor ceramics with a high breakdown voltage.

Following our previous results on Y<sub>2</sub>O<sub>3</sub>-doped varistor ceramics,<sup>6</sup> in this study we report on the influence of the amount of added Sb<sub>2</sub>O<sub>3</sub> on the microstructural, current-voltage (I–V) and capacitance-voltage (C–V) characteristics of ZnO–Bi<sub>2</sub>O<sub>3</sub>-based varistor ceramics doped with Y<sub>2</sub>O<sub>3</sub>.

## 2. Experimental

ZnO–Bi<sub>2</sub>O<sub>3</sub>-based varistor samples with the nominal composition (96.65–*x*) mol% ZnO + 0.9 mol% Bi<sub>2</sub>O<sub>3</sub> + 2.0 mol% (Co<sub>3</sub>O<sub>4</sub> + Mn<sub>3</sub>O<sub>4</sub> + NiO + Cr<sub>2</sub>O<sub>3</sub>) + 0.45 mol% Y<sub>2</sub>O<sub>3</sub> + *x* mol% Sb<sub>2</sub>O<sub>3</sub> for *x* = 1.8, 1.35, 1.0, 0.9, 0.65, 0.45, 0.225 and 0.0 (samples labeled S1.8, S1.35, S1.0, S0.9, S0.65, S0.45, S0.225 and S0, respectively) were prepared by the classical ceramic procedure. For comparison a composition with 1.0 mol% of Sb<sub>2</sub>O<sub>3</sub> and

\* Corresponding author. Tel.: +386-1-4773-682; fax: +386-1-4263-126.

E-mail address: [slavko.bernik@ijs.si](mailto:slavko.bernik@ijs.si) (S. Bernik).

without added  $\text{Y}_2\text{O}_3$  was also prepared (labeled RS). Reagent-grade oxides were mixed in proper ratios and powder mixtures were pressed into discs of 10 mm diameter and 2 mm thick. The pellets were fired at 1230 °C for 2 h in air.

The phase composition of the samples was analyzed by X-ray powder diffraction (XRD) analysis. The samples' microstructures were examined using a scanning electron microscope (SEM) in back-scattered electron (BE) mode. The phase compositions of the samples and the composition of the individual phases were determined by energy-disperse X-ray spectroscopy (EDS) in the SEM. The average ZnO grain size ( $D$ ) was determined for each sample from measurement of 500 to 800 grains per sample.

For the DC current-voltage (I–V) characterisation, silver electrodes were painted on both surfaces of the disk and fired at 590 °C in air. The nominal varistor voltages ( $V_N$ ) at 1 and 10 mA were measured and the threshold voltage  $V_T$  (V/mm) and non-linear coefficient  $\alpha$  were determined. The leakage current ( $I_L$ ) was measured at 0.75  $V_N$  (1 mA).

### 3. Results and discussion

XRD patterns of the investigated samples are presented in Fig. 1. While in the RS sample without added  $\text{Y}_2\text{O}_3$  the ZnO phase, the  $\text{Zn}_7\text{Sb}_2\text{O}_{12}$  spinel phase and the  $\gamma\text{-Bi}_2\text{O}_3$  phase were identified by XRD analysis, in samples co-doped with  $\text{Y}_2\text{O}_3$  and  $\text{Sb}_2\text{O}_3$  the additional peaks of the Bi–Zn–Sb–Y–O ( $\text{Y}_2\text{O}_3$ -containing phase)<sup>6</sup> phase were observed. The XRD peak intensities of the spinel phase decrease with decreasing amount of added  $\text{Sb}_2\text{O}_3$  and in the  $\text{Y}_2\text{O}_3$  doped sample S0 without  $\text{Sb}_2\text{O}_3$

added the spinel phase is absent. Also, no  $\text{Y}_2\text{O}_3$ -containing phase was detected in this sample, while the  $\text{Bi}_2\text{O}_3$  phase was identified as Bi–Y–O phase ( $\text{Bi}_{1.9}\text{Y}_{0.1}\text{O}_3$  phase according to JCPDF 39-0275). In the S0 sample a Zn–Cr–O phase was also detected ( $\text{ZnCrO}_4$  phase according to a JCPDF 19-1456).

BE images from the SEM that reveal the main microstructural characteristics of the varistor samples are given in Figs. 2 and 3. The phases were identified by EDS analysis and the results confirmed the phase composition of the samples already determined by the XRD analysis. In all the  $\text{Y}_2\text{O}_3$ - and  $\text{Sb}_2\text{O}_3$ -doped varistor samples, in addition to the ZnO phase, the  $\text{Zn}_7\text{Sb}_2\text{O}_{12}$  spinel-type phase and the  $\text{Bi}_2\text{O}_3$ -rich phase, the Bi–Zn–Sb–Y–O phase ( $\text{Y}_2\text{O}_3$ -containing phase) was identified at the grain boundaries of the ZnO. It is evident from Fig. 2, and was confirmed by a measurement of the area of the BE images that belongs to the spinel phase, that the amount of spinel phase in the samples decreases with decreasing amounts of added  $\text{Sb}_2\text{O}_3$ . Also, with decreasing amounts of  $\text{Sb}_2\text{O}_3$  the composition of the  $\text{Y}_2\text{O}_3$ -phase alters and contains less Sb. It is evident from Fig. 2 that in sample S1.8, with the largest amount of added  $\text{Sb}_2\text{O}_3$ , the  $\text{Y}_2\text{O}_3$ -containing phase is fine grained and clustered, while it is fine grained and uniformly distributed along the grain boundaries of the  $\text{Y}_2\text{O}_3$ - and  $\text{Sb}_2\text{O}_3$ -doped samples with less added  $\text{Sb}_2\text{O}_3$ . The distribution and morphology of the  $\text{Y}_2\text{O}_3$ -containing phase are clearly evident in Fig. 3a. The  $\text{Y}_2\text{O}_3$ -containing phase is fine grained with grains of micrometer size and less, which is significantly smaller when compared to the grain size of the spinel phase. In sample S0, without added  $\text{Sb}_2\text{O}_3$ , the spinel and the  $\text{Y}_2\text{O}_3$ -containing phase are not present. At the ZnO grain boundaries of this sample the  $\text{Bi}_2\text{O}_3$ -rich phase containing  $\text{Y}_2\text{O}_3$  and ZnO (most probably detected from the neighbouring ZnO grains) was determined by EDS analysis in which small grains of a Zn–Cr–O phase were also identified (Fig. 3b). In the  $\text{Y}_2\text{O}_3$ - and  $\text{Sb}_2\text{O}_3$ -doped samples the grain size can be inhibited by the spinel phase and the  $\text{Y}_2\text{O}_3$ -containing phase. However, despite the decrease in the amount of spinel phase in these samples due to the decrease in the amount of added  $\text{Sb}_2\text{O}_3$  the size of the ZnO grains is rather similar, around 8  $\mu\text{m}$ , in all varistor samples doped with  $\text{Y}_2\text{O}_3$  and  $\text{Sb}_2\text{O}_3$ ; this is except for sample S0.225 with the lowest addition of  $\text{Sb}_2\text{O}_3$  where it is higher, at 10  $\mu\text{m}$ , and is comparable to the grain size of the RS sample without added  $\text{Y}_2\text{O}_3$  (10.4  $\mu\text{m}$ ). Sample RS has a similar amount of spinel phase as sample S1.35 does, and a significantly larger amount of spinel phase than sample S1.0; however, it does not contain the  $\text{Y}_2\text{O}_3$ -containing phase, and hence it has a significantly larger ZnO grain size than the other two samples. The results indicate that a fine-grained  $\text{Y}_2\text{O}_3$ -containing phase that is uniformly distributed along the grain boundaries of the

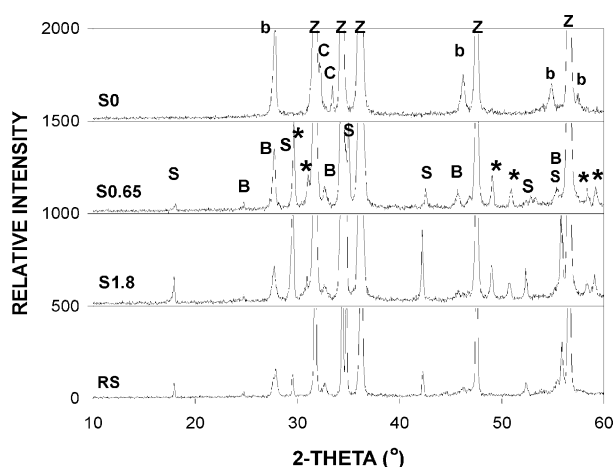


Fig. 1. XRD patterns of ZnO– $\text{Bi}_2\text{O}_3$ -based varistor samples RS, S1.8, S0.65 and S0, fired at 1230 °C for 2 h; Z: ZnO phase, S: spinel phase, B:  $\gamma\text{-Bi}_2\text{O}_3$  phase, b: Bi–Y–O phase, \*:  $\text{Y}_2\text{O}_3$ -containing phase, C: Zn–Cr–O phase.

ZnO inhibits the grain growth very effectively. The ZnO grain size is significantly larger, at 20  $\mu\text{m}$ , in sample S0, because the phases that inhibit ZnO grain growth, namely the spinel phase and the  $\text{Y}_2\text{O}_3$ -containing phase, are absent. The ZnO grains in this sample do not

contain inversion boundaries (IBs), which can influence the grain growth as well.<sup>3,8</sup>

The starting composition does not influence the non-linear coefficient  $\alpha$ , which is 40 for all the samples. The threshold voltage ( $V_T$ ) of the samples strongly correlates

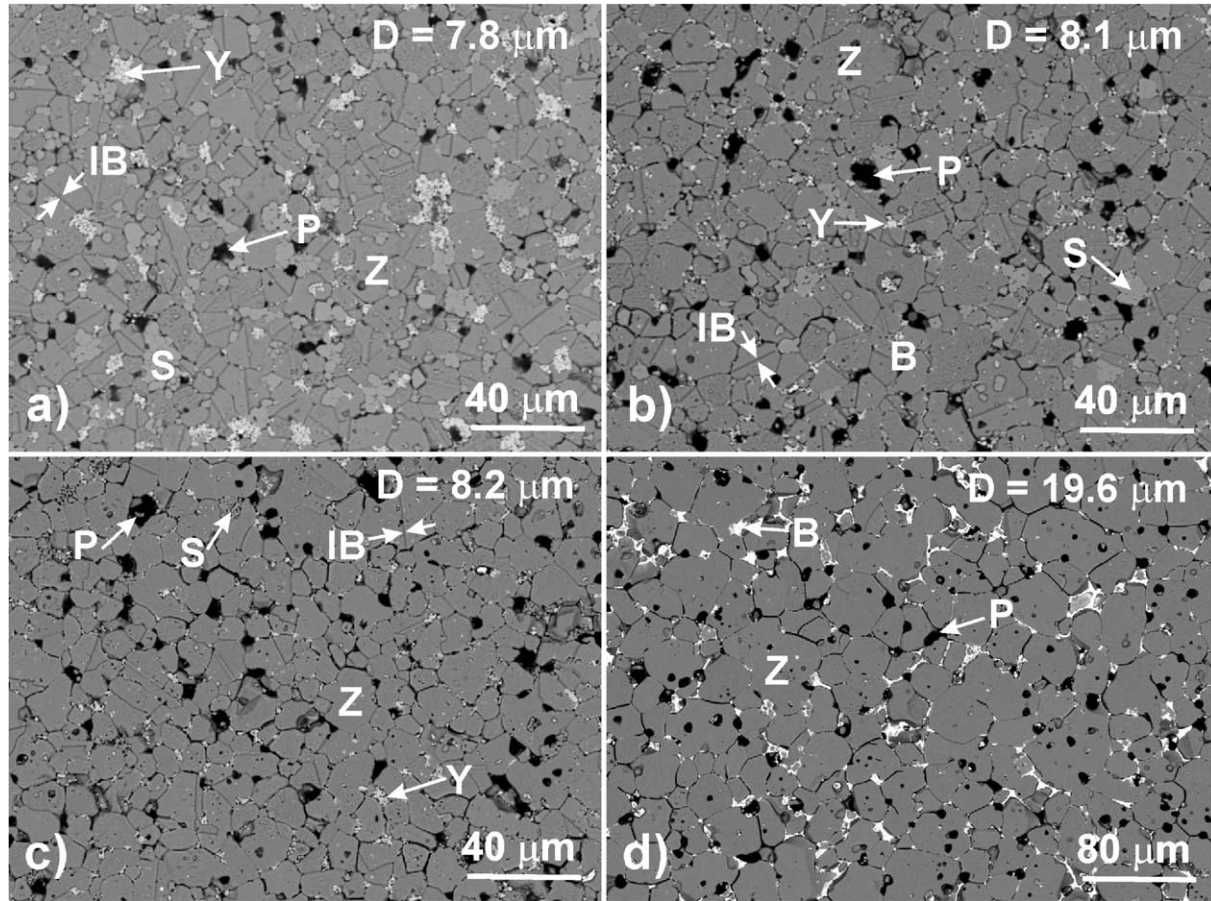


Fig. 2. Backscattered electron (BE) images of varistor samples fired at 1230 °C for 2 h. (a) S1.8, (b) S0.9, (c) S0.45 and (d) S0. Z:  $\text{ZnO}(\text{Co}, \text{Mn})$  phase; S:  $\text{Zn}_7\text{Sb}_2\text{O}_{12}(\text{Cr}, \text{Mn}, \text{Co}, \text{Ni})$  spinel-type phase; B:  $\text{Bi}_2\text{O}_3(\text{Zn}, \text{Y})$  phase; Y:  $\text{Bi-Sb-Zn-Y-O}(\text{Cr}, \text{Mn}, \text{Co}, \text{Ni})$  phase; C:  $\text{Zn-Cr-O}(\text{Mn}, \text{Co}, \text{Ni})$  phase; P: pore; IB: inversion boundary.

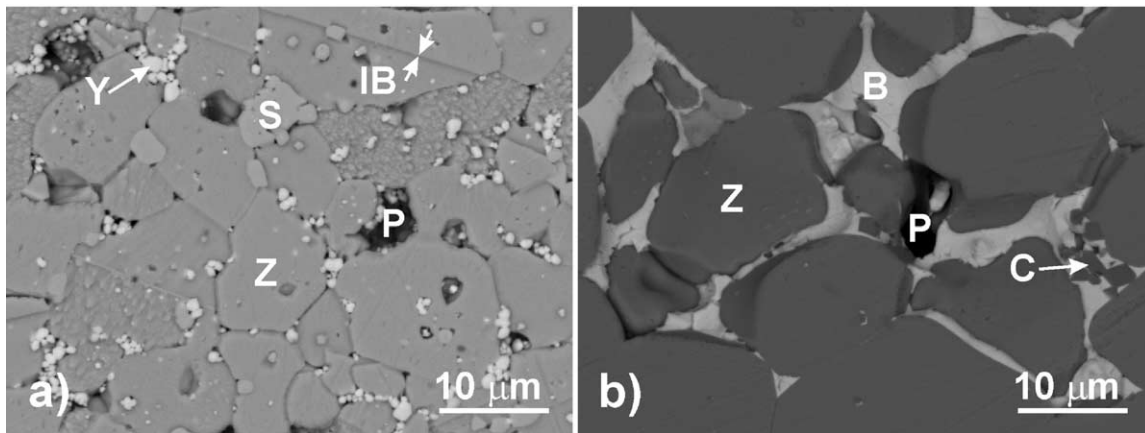


Fig. 3. Backscattered electron (BE) images of varistor samples (a) S0.45 and (b) S0, fired at 1230 °C for 2 h. Z:  $\text{ZnO}(\text{Co}, \text{Mn})$  phase; S:  $\text{Zn}_7\text{Sb}_2\text{O}_{12}(\text{Cr}, \text{Mn}, \text{Co}, \text{Ni})$  spinel-type phase; B:  $\text{Bi}_2\text{O}_3(\text{Zn}, \text{Y})$  phase; Y:  $\text{Bi-Sb-Zn-Y-O}(\text{Cr}, \text{Mn}, \text{Co}, \text{Ni})$  phase; C:  $\text{Zn-Cr-O}(\text{Mn}, \text{Co}, \text{Ni})$  phase; P: pore; IB: inversion boundary.

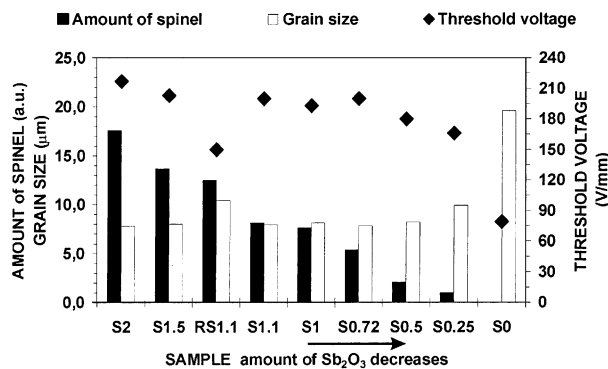


Fig. 4. Influence of the samples composition (amount of  $\text{Sb}_2\text{O}_3$  added) on the amount of spinel phase, the average ZnO grain size and the threshold voltage ( $V_T$ ) of varistor samples, fired at 1230 °C for 2 h.

with the ZnO grain size and is higher in samples with a smaller ZnO grain size, and vice versa. As the ZnO grain size is similar for most of the samples that are doped with  $\text{Y}_2\text{O}_3$  and  $\text{Sb}_2\text{O}_3$  they have similar threshold voltages ( $V_T$ ) of 200 V/mm. The  $V_T$  is slightly higher in sample S1.8, with the largest  $\text{Sb}_2\text{O}_3$  addition of 1.8 mol%, and starts to decrease significantly for amounts of added  $\text{Sb}_2\text{O}_3$  below 0.45 mol%. Correlations between samples' composition, amount of spinel phase, average ZnO grain size and threshold voltage ( $V_T$ ) are graphically presented in Fig. 4. The average breakdown voltage per grain boundary ( $V_{GB}$ ), calculated from  $V_T$  and the average ZnO grain size, is 1.6 V for all samples, which indicates that the starting composition does not influence the fraction of all the grain boundaries in the sample that have non-ohmic characteristics. The leakage current ( $I_L$ ) of the samples is at 0.1  $\mu\text{A}$  for the  $\text{Y}_2\text{O}_3$ -free sample RS and  $\text{Y}_2\text{O}_3$ -doped samples with amount of added  $\text{Sb}_2\text{O}_3$  0.90 mol% and higher. In samples with a lower amount of added  $\text{Sb}_2\text{O}_3$  the  $I_L$  steadily increases and reaches 2.2  $\mu\text{A}$  in sample S0 without added  $\text{Sb}_2\text{O}_3$ . This can be attributed to a weak donor effect of the  $\text{Y}_2\text{O}_3$ <sup>6</sup> and the influence that decreasing the amount of  $\text{Sb}_2\text{O}_3$  has on the distribution of all other varistor dopants along the grain boundaries of ZnO.

#### 4. Conclusions

The influence of the amount of added  $\text{Sb}_2\text{O}_3$  in the starting composition on the characteristics of  $\text{Y}_2\text{O}_3$ -

doped ZnO– $\text{Bi}_2\text{O}_3$ -based varistor ceramics was investigated. In the  $\text{Sb}_2\text{O}_3$ – $\text{Y}_2\text{O}_3$  co-doped samples the spinel and the Bi–Zn–Sb–Y–O phase (the  $\text{Y}_2\text{O}_3$ -containing phase) are present at the grain boundaries and hinder the grain growth. Despite of a decrease in the amount of added  $\text{Sb}_2\text{O}_3$  from 1.8 to 0.45 mol% and a significant decrease in the amount of spinel phase the samples had a similar ZnO grain size and a threshold voltage of 200 V/mm. This indicates that a uniformly distributed and fine-grained  $\text{Y}_2\text{O}_3$ -containing phase is a very effective grain-growth inhibitor. The  $\text{Y}_2\text{O}_3$ -containing phase forms only in the presence of the  $\text{Sb}_2\text{O}_3$ , otherwise the  $\text{Y}_2\text{O}_3$  incorporates into the  $\text{Bi}_2\text{O}_3$ -rich phase and the average ZnO grain size of sample without added  $\text{Sb}_2\text{O}_3$  is more than doubled in comparison to the  $\text{Sb}_2\text{O}_3$ - and  $\text{Y}_2\text{O}_3$ -doped samples.

#### Acknowledgements

The support of the Ministry of Education, Science and Sport of the Republic of Slovenia and the EGIDE society, France, as part of a Slovene-French scientific and technical collaboration is gratefully acknowledged.

#### References

- Clarke, D. R., Varistor ceramics. *J. Am. Ceram. Soc.*, 1999, **82**(3), 485–502.
- Senda, T. and Bradt, R. C., Grain growth of zinc oxide during the sintering of zinc oxide-antimony oxide ceramics. *J. Am. Ceram. Soc.*, 1991, **74**(6), 1296–1302.
- Daneu, N., Recnik, A., Bernik, S. and Kolar, D., Microstructural development in SnO-doped ZnO– $\text{Bi}_2\text{O}_3$  ceramics. *J. Am. Ceram. Soc.*, 2000, **83**(12), 3165–3171.
- Bernik, S., Bernard, J. and Recnik, A. Control of grain growth in  $\text{Sb}_2\text{O}_3$ -doped ZnO ceramics by inversion boundaries. *Abstract Book, 104th Annual Meeting & Exposition*. The American Ceramic Society, 2002, p. 246.
- Shichimiya, S., Yamaguchi, M., Furuse, N., Kobayashi, M. and Ishibe, S., Development of advanced arresters for GIS with new zinc-oxide elements. *IEEE Trans. Power Delivery*, 1998, **13**(2), 465–471.
- Bernik, S., Macek, S. and Bui, A., Microstructural and electrical characteristics of  $\text{Y}_2\text{O}_3$ -doped ZnO– $\text{Bi}_2\text{O}_3$ -based varistor ceramics. *J. Eur. Ceram. Soc.*, 2001, **21**(10–11), 1875–1878.
- Hung, N. T., Quang, N. D. and Bernik, S., Electrical and microstructural characteristics of ZnO– $\text{Bi}_2\text{O}_3$ -based varistors doped with rare-earth oxides. *J. Mater. Res.*, 2001, **16**(10), 2817–2823.
- Recnik, A., Daneu, N., Walther, T. and Mader, W., Structure and chemistry of basal-plane inversion boundaries in antimony oxide doped zinc oxide. *J. Am. Ceram. Soc.*, 2001, **84**(11), 2657–2668.